# Effects of semiclassical spiral fluctuations on hole dynamics

I. J. Hamad, L. O. Manuel, and A. E. Trumper
*Instituto de Física Rosario (CONICET) and Universidad Nacional de Rosario, Boulevard 27 de Febrero 210 bis, (2000) Rosario, Argentina*
(Received 12 September 2011; revised manuscript received 10 November 2011; published 4 January 2012)

We investigate the dynamics of a single hole coupled to the spiral fluctuations related to the magnetic ground states of the antiferromagnetic $J_1$-$J_2$-$J_3$ Heisenberg model on a square lattice. Using exact diagonalization on finite size clusters and the self-consistent Born approximation in the thermodynamic limit, we find, as a general feature, a strong reduction of the quasiparticle weight along the spiral phases of the magnetic phase diagram. For an important region of the Brillouin zone the hole spectral functions are completely incoherent, whereas at low energies the spectral weight is redistributed on several irregular peaks. We find a characteristic value of the spiral pitch $\mathbf{Q} = (0.7,0.7)\pi$, for which the available phase space for hole scattering is maximum. We argue that this behavior is due to the nontrivial interference of the magnon-assisted and the free-hopping mechanism for hole motion, characteristic of a hole coupled to semiclassical spiral fluctuations.

DOI: 10.1103/PhysRevB.85.024402 PACS number(s): 75.50.Ee, 71.10.Fd

## I. INTRODUCTION

The interplay between charge and spin degrees of freedom in a 2D doped Mott insulator represents an important problem in condensed matter physics.[1,2] The strong constraint on the double occupancy gives rise to the nontrivial coupling of the charge motion with the magnetic background, which is believed to be well described by the $t$-$J$ model. In this context, Shraiman and Siggia[3] showed that hole motion produces a long-range dipolar distortion of the staggered magnetization resulting in a spiral order characterized by a pitch proportional to hole doping. Further studies focused on the spiral stability under low doping[4] and its possible relation with the spin glass behavior found in the superconducting cuprates. Regarding the charge dynamics, much interest was concentrated on the possibility of extending the concept of quasiparticle excitation in hole doped antiferromagnets (AF). In fact, it was suggested that already for the one hole case the distortion of the magnetic background would lead to an orthogonality catastrophe,[5] signaled by the vanishing of the quasiparticle (QP) weight $z_{\mathbf{k}}$. Subsequent works,[6] however, showed that such a dipolar distortion is compatible with a coherent quasiparticle excitation with a finite $z_{\mathbf{k}}$. Furthermore, a semiclassical treatment of the magnetic background, based on the linear spin wave theory (LSWT), captures the main features of the QP excitation which can be envisaged as a bare hole surrounded by an AF cloud.[6] This interpretation of the low-lying excitation has been coined the spin polaron picture, due to the analogy with the phononic polaron problem, and for unfrustrated AF it seems to be valid for the whole Brillouin zone (BZ).

When frustration is present in the undoped AF, the hole dynamics may change significantly due to the stabilization of more complex magnetic ground states. For instance, already in the 120° Néel ground state of the triangular antiferromagnet (AF), the validity of the spin polaron picture depends crucially[7] on the sign of the hopping $t$ for an important region of the BZ, while for the kagomé AF the hole spectral functions seem to be completely incoherent[8] for the whole BZ. This behavior has been attributed to the presence of an exponentially large number of singlet excitations inside the triplet gap.[9] Therefore, the coupling of the hole with the underlying excitations above the magnetic ground state is crucial.

Very recently, the phase diagram of the $J_1$-$J_2$-$J_3$ model was studied exhaustively with functional renormalization group, coupled cluster method, and series expansion.[10] The good agreement among these complementary techniques allowed us to establish the location of the quantum disordered (QD) regime in an important region of the parameter space (see right panel of Fig. 1). Furthermore, in this QD regime substantial plaquette and short-range incommensurate spiral fluctuations were found, in agreement with early exact diagonalization studies on finite systems.[11] Consequently, it is interesting to investigate whether the spin polaron picture is still valid within the QD regime of the model.

Motivated by this issue, we investigate, as a first step, the spectral function of a hole coupled to the spiral fluctuations of the $J_1$-$J_2$-$J_3$ model. Using the $t$-$J$ model, solved with exact diagonalization and within the self-consistent Born approximation (SCBA),[12,13] we found that (i) for some regimes the sole inclusion of semiclassical spiral fluctuations in the SCBA is enough to describe quite well the exact hole spectral functions on finite systems and (ii) in the thermodynamic limit the QP coherence is lost, due to the strong interference of the magnon-assisted and the free-hopping mechanisms for hole motion of the effective Hamiltonian, which increases the available phase space for hole scattering. In fact, at low energies the spectral weight is redistributed on several irregular peaks, or multipoles. On the other hand, in the weak coupling regime ($J_1/t \sim 10$), where only a few magnons are involved, we have found an important area of the parameter space of the model where the quasiparticle weight averaged on the entire BZ is $z_{av} \lesssim 0.6$ (see shaded area of Fig. 5), in contrast to the expected value $z_{av} \sim 1$ for this regime. By fine tuning frustration, we found that the loss of QP coherence is maximum when the magnetic pitch is around $\mathbf{Q} = (0.7\pi,0.7\pi)$. In many cases, this spiral pitch corresponds to quite well ordered spirals. Therefore, we can suggest that the breakdown of the spin polaron picture, signaled by the QP vanishing, is a direct consequence of the hole coupled with semiclassical spiral fluctuations.

 

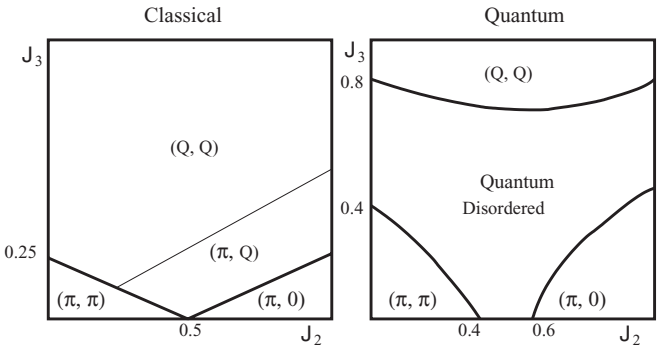


FIG. 1. Phase diagram of the $J_1$-$J_2$-$J_3$ model. Left panel is the classical one with the magnetic phases characterized by the spiral pitch indicated in parenthesis (Ref. 10). Right panel: sketch of the quantum phase diagram for $S = \frac{1}{2}$ recently found in Ref. 10.

The paper is organized as follows: In Sec. II A, we briefly resume the magnetic phase diagram of the $J_1$-$J_2$-$J_3$ model along with the LSW calculation. In Sec. II B, we present the $t$-$J$ model treated within the self-consistent Born approximation. In Sec. III, we compare the spectra predicted by the SCBA with exact diagonalization on finite clusters and analyze the spectra in the thermodynamic limit. In Sec IV, we close with the conclusions.

## II. MODELS AND METHODS

### A. $J_1$-$J_2$-$J_3$ model

The $J_1$-$J_2$-$J_3$ AF Heisenberg model on a square lattice is defined as

$$H_J = J_1 \sum_{\langle ij \rangle} \mathbf{S}_i \cdot \mathbf{S}_j + J_2 \sum_{\langle ik \rangle} \mathbf{S}_i \cdot \mathbf{S}_k + J_3 \sum_{\langle im \rangle} \mathbf{S}_i \cdot \mathbf{S}_m, \qquad (1)$$

where $\langle ij \rangle$, $\langle ik \rangle$, and $\langle im \rangle$ indicate sums to first, second, and third neighbors, respectively. The classical phase diagram of this model is shown in the left panel of Fig. 1 and contains *Nèel* $(\pi,\pi)$, *spirals* $(Q,Q)$ and $(Q,\pi)$, and *collinear* $(\pi,0)$ or $(0,\pi)$ phases.[14] The thick and thin lines indicate continuous and discontinuous transitions, respectively. Actually, the collinear $(\pi,0)$ and $(0,\pi)$ phases are degenerated with an infinite number of interpenetrating Néel states, but it is known that quantum fluctuations select the collinear ones by the well-known *order by disorder* phenomenon.[15]

For spin $S = \frac{1}{2}$, a semiclassical spin wave study predicts an intermediate disordered phase along the classical transition lines between the classical phases.[14] For a long time, the quantum $S = \frac{1}{2}$ case of the $J_1$-$J_2$ model has been intensively studied in the literature.[16] Only recently, however, the complete quantum phase diagram has been investigated with more sophisticated techniques. In the right panel of Fig. 1, a sketch of the quantum phase diagram of the recently found model for $S = \frac{1}{2}$ is displayed.[10] In particular, in the quantum disordered regime there is evidence of short-range plaquette and incommensurate spiral correlations. As we have mentioned in the introduction, in the present work we will consider the effects of the spiral fluctuations on the single-hole dynamics and leave the effects of plaquette fluctuations for a future work. Since the hole dynamics is sensitive to short-range character of the magnetic fluctuations, and given that the spiral pitch values practically coincide with the classical ones,[10] we assume the magnetic background within the semiclassical linear spin wave theory. For spiral phases, the spin operators of $H_J$ [Eq. (1)] are expressed with respect to a *local axis* pointing in the classical direction of the spin at each site. Using the Holstein-Primakoff transformation in Eq. (1), the following quadratic Hamiltonian results:

$$\hat{H}_J = \sum_{\mathbf{q}} \gamma_{\mathbf{q}} \hat{a}^\dagger_{\mathbf{q}} \hat{a}_{\mathbf{q}} + \frac{1}{2} \sum_{\mathbf{q}} \beta_{\mathbf{q}} (\hat{a}^\dagger_{\mathbf{q}} \hat{a}^\dagger_{-\mathbf{q}} + \hat{a}_{-\mathbf{q}} \hat{a}_{\mathbf{q}}) + E_{cl}, \qquad (2)$$

where

$$\gamma_{\mathbf{q}} = 2s \sum_{\delta>0} J_\delta \left[ \cos^2 \frac{\mathbf{Q}.\delta}{2} \cos \mathbf{q}.\delta - \cos \mathbf{Q}.\delta \right], \qquad (3)$$

$$\beta_{\mathbf{q}} = -2s \sum_{\delta>0} J_\delta \left[ \sin^2 \frac{\mathbf{Q}.\delta}{2} \cos \mathbf{q}.\delta \right]. \qquad (4)$$

$\mathbf{Q}$ is the spiral pitch that minimizes $J_{\mathbf{k}} = \sum_\delta J_\delta e^{i\mathbf{k}.\delta}$ with the sums on $\delta$ extending up to third neighbors. After Bogoliubov transformation $\hat{a}_{\mathbf{q}} = u_{\mathbf{q}} \hat{\alpha}_{\mathbf{q}} + v_{\mathbf{q}} \hat{\alpha}^\dagger_{-\mathbf{q}}$, such as $u_{\mathbf{q}} = [\frac{\gamma_{\mathbf{q}}+\omega_{\mathbf{q}}}{2\omega_{\mathbf{q}}}]^{\frac{1}{2}}$ and $v_{\mathbf{q}} = -\mathrm{sign}(\beta_{\mathbf{q}})[\frac{\gamma_{\mathbf{q}}-\omega_{\mathbf{q}}}{2\omega_{\mathbf{q}}}]^{\frac{1}{2}}$, the Hamiltonian is diagonalized as

$$\hat{H}_J = \sum_{\mathbf{q}} \omega_{\mathbf{q}} \hat{\alpha}^\dagger_{\mathbf{q}} \hat{\alpha}_{\mathbf{q}} + \frac{1}{2} \sum_{\mathbf{q}} \omega_{\mathbf{q}} + \left(1 + \frac{1}{s}\right) E_{cl.}, \qquad (5)$$

with a magnon relation dispersion

$$\omega^2_{\mathbf{q}} = s^2 [J_{\mathbf{q}} - J_{\mathbf{Q}}] \left[ \tfrac{1}{2} (J_{\mathbf{q}+\mathbf{Q}} + J_{\mathbf{q}-\mathbf{Q}}) - J_{\mathbf{Q}} \right] = \gamma^2_{\mathbf{q}} - \beta^2_{\mathbf{q}}. \qquad (6)$$

While the first member is the usual expression used in the literature for the spin wave dispersion,[14] the second one, in terms of functions $\gamma_{\mathbf{q}}$ and $\beta_{\mathbf{q}}$ allows us to write down a more compact expression for the hole-magnon vertex interaction (see below). Notice that besides the three Goldstone modes at $\mathbf{q} = (0,0)$ and $\mathbf{Q} = \pm(Q,Q)$, corresponding to the complete SO(3) symmetry rupture, at the linear spin wave level, two extra zero modes appear at $\mathbf{k} = (-Q,Q)$ and $(Q,-Q)$ that reflect the lattice symmetry in the spectrum [Eq. (6)]. In fact, a classical spiral $(Q,Q)$ is related to $(Q,-Q)$ and $(-Q,Q)$ by a global rotation combined with a reflexion about the $y$ and $x$ axis, respectively.[17] Higher orders beyond linear spin wave theory will lift these degeneracies;[18] nevertheless, for our purposes, it is enough to keep up to quadratic order since the main effects on the hole dynamics will be related to the noncollinearity of the magnetic background characterized by the spiral pitch $\mathbf{Q}$ (see below).

### B. $t$-$J$ model and SCBA

The dynamics of a hole coupled with the magnetic excitations of a Mott insulator is properly described by the $t$-$J$ model[2] defined as

$$H_{t\text{-}J} = H_t + H_J = -t \sum_{\langle ij \rangle \sigma} (\tilde{c}^\dagger_{i\sigma} \tilde{c}_{j\sigma} + \mathrm{H.c.}) + H_J, \qquad (7)$$

where the electronic operators are the projected ones, $\tilde{c}_{i\sigma} = (1 - n_{i-\sigma}) c_{i\sigma}$, that obey the no double occupancy constraint, and in our present case $H_J$ is Eq. (1). To take care of the

constraint, we use the spinless fermion representation[12] for $H_t$, leading to the following effective Hamiltonian for the hole

$$H_{\rm eff} = \sum_{\mathbf{k}} \epsilon_{\mathbf{k}} h^{\dagger}_{\mathbf{k}} h_{\mathbf{k}} + \frac{2s}{\sqrt{N}} \sum_{\mathbf{k},\mathbf{q}} (M_{\mathbf{k},\mathbf{q}} \hat{h}^{\dagger}_{\mathbf{k}-\mathbf{q}} \hat{h}_{\mathbf{k}} \alpha^{\dagger}_{\mathbf{q}} + \text{H.c.}). \quad (8)$$

The first term of Eq. (8) describes the free hopping of the hole without disturbing the magnetic background, and is characterized by the hole dispersion $\epsilon_{\mathbf{k}} = 2s \sum_{\boldsymbol{R}>0} 2t_{\boldsymbol{R}} \cos(\frac{\mathbf{Q}\cdot\boldsymbol{R}}{2}) \cos(\mathbf{k}\cdot\boldsymbol{R})$ with $\boldsymbol{R} = (1,0),(0,1)$, in units of lattice space $a$. The second term describes the magnon-assisted mechanism for the hole motion, and is characterized by the hole-magnon vertex

$$M_{\mathbf{kq}} = \imath(\eta_{\mathbf{k}-\mathbf{q}} u_{\mathbf{q}} - \eta_{\mathbf{k}} v_{\mathbf{q}}), \quad (9)$$

where $\eta_{\mathbf{k}} = 2s \sum_{\boldsymbol{R}>0} 2t_{\boldsymbol{R}} \sin(\frac{\mathbf{Q}\cdot\boldsymbol{R}}{2}) \sin(\mathbf{k}\cdot\boldsymbol{R})$.

For the Néel phase $\mathbf{Q} = (\pi,\pi)$, the only source involved for hole motion is the magnon-assisted mechanism, owing to the vanishing of the hole dispersion $\epsilon_{\mathbf{k}} = 0$. Nonetheless, it is known that the string of overturned spins generated by this mechanism is partially erased by the zero-point AF spin fluctuations, leading to a coherent propagation of the hole surrounded by an AF cloud. This is the spin polaron picture that is widely accepted in the literature.[12,13] For spiral phases, instead, the free-hopping processes interfere with the magnon-assisted ones. This feature is counter intuitive if one compares it with the usual polaron problem where a free band is renormalized by phonons. In particular, we will show that the interference depends strongly on the spiral pitch $\mathbf{Q}$, which for certain values of frustration leads to the vanishing of $z_{\mathbf{k}}$. Regarding the hole-magnon vertex, it is interesting to note that while for the Néel phase $M_{\mathbf{kq}}$ vanishes at $\mathbf{q} = (0,0)$ and $(\pi,\pi)$, for spiral phases it behaves as

$$M_{\mathbf{kq}} \simeq -2\imath \left[\frac{\gamma_{\mathbf{0}}}{2\omega_{\mathbf{q}}}\right]^{\frac{1}{2}} \sum_{R>0} t_R \ (\mathbf{q}\cdot\mathbf{R}) \ \sin\frac{\mathbf{Q}.\mathbf{R}}{2} \ \cos\mathbf{k}\cdot\mathbf{R} \quad (10)$$

$$M_{\mathbf{k},\mathbf{Q}+\mathbf{q}} = 2\imath \left[\frac{\gamma_{\mathbf{Q}}}{2\omega_{\mathbf{Q}+\mathbf{q}}}\right]^{\frac{1}{2}} \sum_{R>0} t_R \sin\mathbf{Q}.\mathbf{R} \ \sin\left(\mathbf{k} - \frac{\mathbf{Q}}{2}\right)\cdot\mathbf{R} \quad (11)$$

for small $\mathbf{q}$. As $\omega_{\mathbf{q}} \sim |\mathbf{q}|$ and $\omega_{\mathbf{Q}+\mathbf{q}} \sim |\mathbf{q}|$, the above vertices behave as $M_{\mathbf{kq}} \propto |\mathbf{q}|^{\frac{1}{2}}$ and $M_{\mathbf{k},\mathbf{Q}+\mathbf{q}} \propto |\mathbf{q}|^{-\frac{1}{2}}$ around $(0,0)$ and $(Q,Q)$, respectively. To investigate the hole dynamics, we compute the hole spectral function $A_{\mathbf{k}}(\omega) = -(1/\pi)\text{Im}G^h_{\mathbf{k}}(\omega)$, where $G^h_{\mathbf{k}}(\omega) = \langle AF|h_{\mathbf{k}}[1/(\omega + i\eta^+ - H_{\rm eff})]h^{\dagger}_{\mathbf{k}}|AF\rangle$ is the retarded hole Green function, and $|AF\rangle$ is the undoped magnetic ground state in the LSW approximation. In the SCBA, the hole self-energy is given by the following self-consistent equation:[7,12,13]

$$\Sigma_{\mathbf{k}}(\omega) = \sum_{\mathbf{q}} \frac{|M_{\mathbf{kq}}|^2}{\omega + i\eta^+ - \omega_{\mathbf{q}} - \varepsilon_{\mathbf{k}-\mathbf{q}} - \Sigma_{\mathbf{k}-\mathbf{q}}(\omega - \omega_{\mathbf{k}-\mathbf{q}})}, \quad (12)$$

which must be solved numerically. The QP spectral weight can be calculated as

$$z_{\mathbf{k}} = [1 - \partial\Sigma_{\mathbf{k}}(\omega)/\partial\omega]^{-1}|_{E_{\mathbf{k}}}, \quad (13)$$

where the QP energy is given by the equation $E_{\mathbf{k}} = \epsilon_{\mathbf{k}} + \text{Re}\Sigma_{\mathbf{k}}(E_{\mathbf{k}})$.

## III. RESULTS: SCBA AND LANCZOS

### A. Finite systems

In this subsection, we compare the hole spectral functions predicted by the SCBA and exact diagonalization on a cluster size of $N = 20$ sites. For collinear phases $(\pi,\pi)$ and $(\pi,0)$, we have already confirmed in a previous work a very good agreement between both techniques for the hole dynamics in the context of the $J_1$-$J_2$ model.[19] Here we are interested in frustration values that induce spiral correlations. In previous exact studies of the $J_1$-$J_2$-$J_3$ model,[11] a coexistence of spiral and plaquette fluctuations has been shown,which, in principle, would couple with the hole. Therefore, a careful comparison of the exact hole spectral functions with that of the SCBA would allow us to discern the relevance, or lack thereof, of the spiral fluctuations. It is worth stressing that for finite systems the parameter space is restricted to frustration values that give rise to spiral pitch values coincident with the momenta of the $N = 20$ BZ. Even in this case, the strong finite size quantum fluctuations renormalize the classical magnetic wave vector $\mathbf{Q}_{cl}$. So, in order to perform a faithful comparison, we have assumed the position $\mathbf{q}_m$ of the maximum exact structure factor $S(\mathbf{q})$ as the actual spiral pitch characterizing the magnetic background within the SCBA. In Fig. 2, the comparison of the hole spectral functions with Lanczos and SCBA in the strong coupling regime, $J_1/t = 0.4$, is shown, along with the exact structure factor for different values of $J_3/J_1$ at constant values of $J_2$ and hole momentum $\mathbf{k}_{\rm hole}$. It can be seen that the agreement is reasonably good. In particular, when the magnetic structure factor is characterized by only one main peak such as that at $\Delta = (\frac{3}{5}\pi,\frac{4}{5}\pi)$ (see upper panels of Fig. 2), the agreement is quite good, in contrast to the case of two peaks [see $\Delta$ and $X = (\pi,\pi)$ in the lower panels of Fig. 2]. The latter is related to the strong competence of spiral and Néel fluctuations for this regime; however, in the SCBA only the main spiral peak at momentum $\Delta$ is considered. Given that the exact results incorporate all kind of magnetic fluctuations, our results suggest that to describe the main features of the hole spectral function, at least in the regimes considered, it is enough to take into account the coupling of the hole with magnonic excitations above the spiral correlations. In addition, in the spiral regime there is a strong reduction of the quasiparticle weight in the low-energy sector of the above spectra. This issue will be studied in the next subsection for the thermodynamic limit.

### B. Thermodynamic limit

We have computed the hole spectral functions for cluster sizes up to 1600 sites. In complete agreement with previous works, we found that for the frustrated Néel $(\pi,\pi)$ regime the hole spectral functions show a coherent low-energy peak for the whole BZ, which is identified with a well-defined quasiparticle excitation, i.e., spin polaron. This is shown in the dashed line of Fig. 3, where we have plotted the $A(\mathbf{k},\omega)$ for a hole with momentum $\mathbf{k}_{\rm hole} = (0.8\pi,0.8\pi)$ at point $A$ of the magnetic phase diagram (see Fig. 5). For

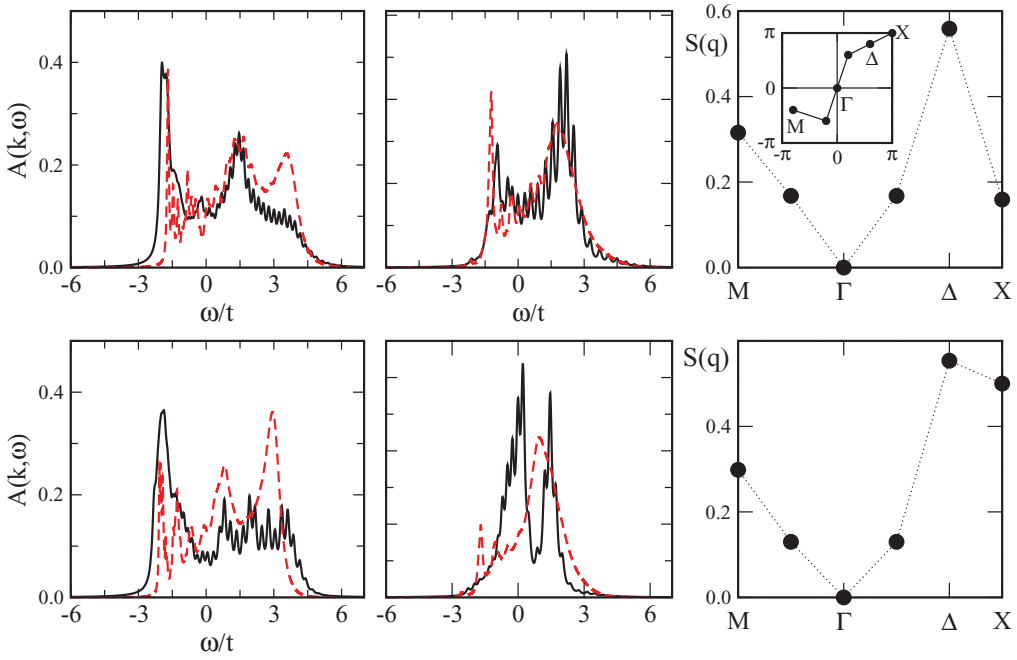


FIG. 2. (Color online) Lanczos (continuous) vs SCBA (dashed) hole spectral functions for a 20 site cluster, momentum $k_{\text{hole}} = (0,\pi)$ (left panels) and $k_{\text{hole}} = (0,0)$ (middle panels), and $J_2/J_1 = 0.2$, $J_1/t = 0.4$. Upper (lower) panels correspond to $J_3/J_1 = 1.5$ ($J_3/J_1 = 0.45$). Right panels: Exact static structure factor $S(\mathbf{q})$. In the SCBA calculation, the magnetic wave vector $\mathbf{Q}$ corresponding to the highest value of $S(\mathbf{q})$ in the exact calculation has been chosen. $M = -(0.8,0.4)\pi$, $\Delta = (0.8,0.6)\pi$, and $\Gamma = (0,0)$.

this case, the QP weight is around $z_{\mathbf{k}} \sim 0.2$, which means a considerable contribution of multimagnon processes to the spin polaron wave function. As frustration increases, the magnon dispersion bandwidth decreases, allowing the hole to emit and absorb magnons more easily.[19] Then, there is an increasing contribution of the multimagnon processes in the spin polaron wave function, accompanied by a reduction of the quasiparticle weight. Therefore, as quantum fluctuations are enhanced by frustration, the QP weight and the magnetization decrease monotonically. It can be seen that the QP weight remains finite even when long-range order is destroyed, which confirms the idea that the hole dynamic is more sensitive to the short-range magnetic fluctuations.

In the incommensurate spiral phase, we have found that the hole spectral functions are completely incoherent for an important region of the BZ. This is shown in the solid line of Fig. 3 where it is plotted $A(\mathbf{k},\omega)$ at point $B$ of the magnetic phase diagram (see Fig. 5) for the same $\mathbf{k}_{\text{hole}}$. In the inset of Fig. 3, the peculiar structure of the low-energy sector which is composed by several irregular peaks where no signal of QP excitation is present is shown. In the SCBA, this feature of the hole spectral function is typical for incommensurate spiral correlations and is related to the fact that there are two mechanisms for hole motion—the magnon assisted and the free one—whose interference may increase the available phase space for hole scattering, leading to the loss of QP excitations. In fact, this effect depends strongly on the spiral pitch which can be fine tuned by frustration. For instance, we have found that when the spiral pitch is around $\mathbf{Q} = (0.7,0.7)\pi$, the effect is maximum with a vanishing of the QP weight in approximately 50% of the BZ. Given that here the local magnetization of the spiral state is about $m \sim 0.24$, one can conclude that the nontrivial hole dynamics is already present at a semiclassical level. We have found a similar behavior for a hole injected in other noncollinear magnetic backgrounds such as the 120° Néel order[7] and canted Néel phases,[20] although the incommensurate spiral correlations seems to be more effective in destroying the QP excitations. It is worth noting that the strong reduction of the QP weight along with the rapid redistribution of the spectral weight on several multipoles has been observed previously on finite systems. Alternatively, these features were related to a scenario of

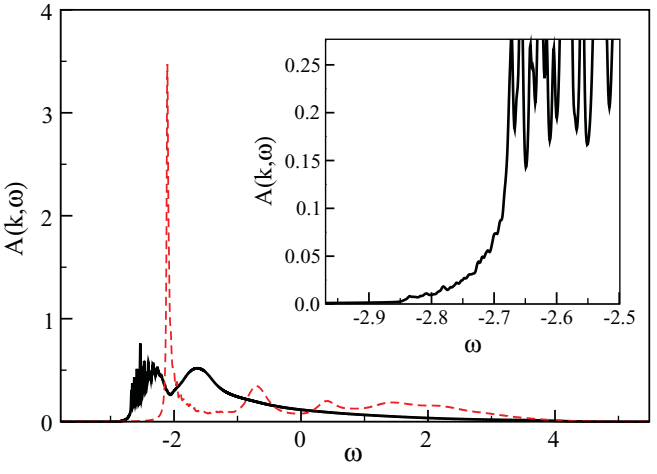


FIG. 3. (Color online) Hole spectral functions obtained by SCBA for 1600 sites, $k_{\text{hole}} = (0.8,0.8)\pi$, $J_2 = 0$, and $J_1/t = 0.4$. Dashed (red) line: $J_3/J_1 = 0.1$ (Neel phase). Continuous line: $J_3/J_1 = 0.425$ [spiral phase, $Q = (0.7,0.7)\pi$]. Inset: low energy sector is zoomed.

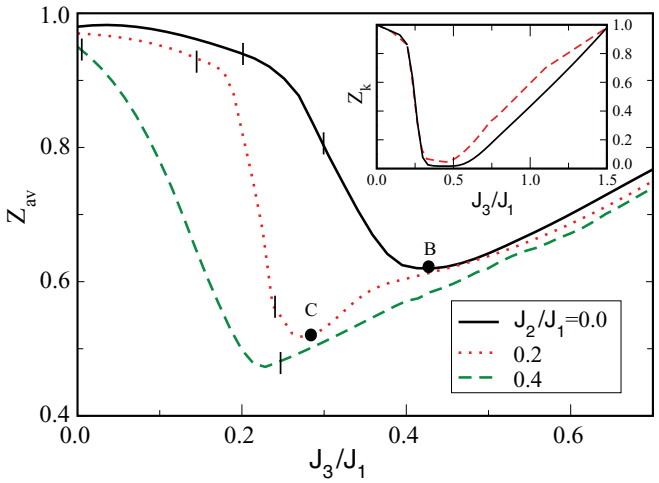


FIG. 4. (Color online) QP weight averaged on the entire BZ, $z_{av} = (1/N)\sum_{\mathbf{k}} z_{\mathbf{k}}$, as a function of $J_3/J_1$, predicted by the SCBA for 1600 sites in the weak coupling regime, $J_1/t = 10$. In between the vertical lines $m = 0$ within the LSW approximation. The dots $B$ and $C$ indicate the values of frustration for which $\mathbf{Q} \approx (0.7,0.7)\pi$ (they are displayed in the magnetic phase diagram of Fig. 5). Inset: QP weight for $\mathbf{k}_{\text{hole}} = (0.3,0.3)\pi$ computed with the SCBA (solid line) and Eq. (14) (dashed line).

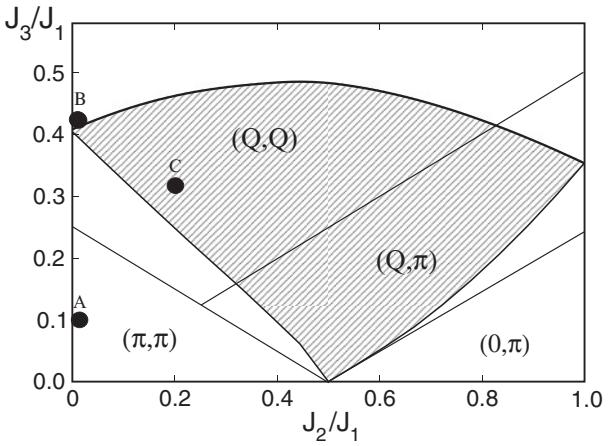


FIG. 5. The shaded area indicates the region of the magnetic phase space where the averaged quasiparticle weight $z_{av} \lesssim 0.6$ in the weak coupling regime ($J_1/t = 10$). For the strong coupling regime, $J_1/t = 0.4$, the SCBA predicts the vanishing of $z_{\mathbf{k}}$ in some area of the BZ. Dots $A = (0,0.1)$, $B = (0,0.425)$, and $C = (0.2,0.32)$ correspond to the frustration values used in Figs. 3 and 4, respectively.

spinon deconfinement[21] which, of course, is out of the scope of our present approximation.

We have further investigated the effect of spiral fluctuations for the very weak coupling regime ($J_1/t \gg 1$). For a Néel phase, the only mechanism for hole motion is magnon assisted, and, owing to its high energy cost, it is expected that the hole reaches a quasistatic regime where the QP weight approaches unity. For spiral phases, however, the hole can move via the free hopping term of Eq. (8), reducing the QP weight even with a very low average number of magnons promoted. Then, in the weak coupling regime, $z_{\mathbf{k}}$ can be approximated by perturbative theory as[12,19]

$$z_{\mathbf{k}} \approx \frac{1}{1+\sum_{\mathbf{q}}[M_{\mathbf{k},\mathbf{q}}/(\epsilon_{\mathbf{k}} - \epsilon_{\mathbf{k}-\mathbf{q}} - \omega_{\mathbf{q}})]^2}, \qquad (14)$$

where the QP dispersion $E_{\mathbf{k}}$ has been replaced by the bare dispersion $\epsilon_{\mathbf{k}}$. In the inset of Fig. 4, the good agreement between Eq. (14) (dashed line) and the QP weight computed with Eq. (13) (solid line) for different values of frustration is shown. In particular, for the selected hole momentum, $z_{\mathbf{k}}$ is strongly reduced once the magnetic background reaches the spiral regime. In principle, one can attribute the reduced value of $z_{\mathbf{k}}$ for spiral phases to the vertex behavior near $(Q,Q)$, $M_{\mathbf{k},\mathbf{Q}+\mathbf{q}} \propto |\mathbf{q}|^{-\frac{1}{2}}$. Nonetheless, we have checked that the most important contribution comes from the small values assumed by the denominators $\epsilon_{\mathbf{k}} - \epsilon_{\mathbf{k}-\mathbf{q}} - \omega_{\mathbf{q}}$. In order to quantify globally this behavior, we have plotted in Fig. 4 the QP spectral weight averaged on the entire BZ, $z_{av} = (1/N)\sum_{\mathbf{k}} z_{\mathbf{k}}$, for $J_1/t = 10$. Again, it can be observed that as $J_3/J_1$ increases, $z_{av}$ decreases notably when the magnetic background reaches the spiral regime. In particular, for $J_2/J_1 < 0.5$, a single minimum at $\mathbf{Q} \approx (0.7,0.7)\pi$ is always observed, analogous to that found in the strong coupling regime (Fig. 3). For $J_2/J_1 = 0$ (continuous line in Fig. 4), $\mathbf{Q}$ occurs in a region where $m \approx 0.24$, while for $J_2/J_1 = 0.4$ (dashed line), $\mathbf{Q}$ is inside the region where $m = 0$. In the latter, we have modified the LSW approximation by introducing a gap in the magnetic dispersion in order to describe the short-range spiral order properly.[22]

In order to show that the strong reduction of the QP weight is a general feature of the subtle coupling of the hole with the spiral magnetic fluctuations, we have studied the hole spectral functions for an important region of the magnetic phase diagram. The shaded area of Fig. 5 indicates the region of the magnetic phase diagram where the averaged QP weight is $z_{av} \lesssim 0.6$ for the very weak coupling regime. Notice that in this regime, one would expect a value of $z_{av} \sim 1$, as occurs within the Néel $(\pi,\pi)$ and the Collinear $(0,\pi)$ phases.[19] Since this behavior is independent of the range of the magnetic fluctuations, we expect the same effect for a hole coupled to the short-range spiral fluctuation of the actual quantum magnetic phase diagram (see right panel of Fig. 1).

## IV. CONCLUSIONS

We have investigated the effect of semiclassical spiral fluctuations on single hole dynamics. Based on the magnetic phase diagram of the $J_1$-$J_2$-$J_3$ model, and solving the hole Green function with exact diagonalization and within the SCBA, we found that for the weak ($J_1/t \gg 1$) and the strong ($J_1/t \leqslant 1$) coupling regime there is a characteristic value of the spiral pitch $\mathbf{Q} \approx (0.7,0.7)\pi$, for which the available phase space for hole scattering is maximum. Notably, for the whole spiral regimes [$(Q,Q)$ and $(Q,\pi)$] of the model, we found a strong reduction of the averaged QP weight $z_{av}$. In particular, for some momenta the QP weight vanishes and the spectral weight at low energy is redistributed on several irregular peaks, or multipoles. Even if in our study the spirals have been described semiclassically; we think that this effect should be also observed in the short-range spiral phases recently found in the disordered regime of the quantum phase diagram.[10]

Similar features have been found in finite size studies of the same model, although the strong reduction of the QP weight has been attributed to the spinon deconfinement inherent of the plaquette fluctuations.[21] Based on our results and given that the alternative scenario for spinon deconfinement is based on short-range spiral correlations,[23] it would be important to go beyond the semiclassical description and investigate, within the context of the present model, the hole dynamics on spirals treated in terms of spinon excitations.[24] Work in this direction is in progress.

## ACKNOWLEDGMENTS

We thank A. E. Feiguin for his valuable help and useful discussions. This work was supported by CONICET under Grant PIP2009 N 1948.

[1]E. Dagotto, Rev. Mod. Phys. **66**, 763 (1994).
[2]P. A. Lee, N. Nagaosa, and X. G. Wen, Rev. Mod. Phys. **78**, 17 (2006).
[3]B. I. Shraiman and E. D. Siggia, Phys. Rev. Lett. **62**, 1564 (1989); Phys. Rev. B **46**, 8305 (1992).
[4]O. P. Sushkov and V. N. Kotov, Phys. Rev. B **70**, 024503 (2004), and references therein.
[5]P. W. Anderson, Phys. Rev. Lett. **64**, 1839 (1990).
[6]G. F. Reiter, Phys. Rev. B **49**, 1536 (1994); A. Ramsak and P. Horsch, *ibid.* **57**, 4308 (1998).
[7]A. E. Trumper, C. J. Gazza, and L. O. Manuel, Phys. Rev. B **69**, 184407 (2004); Physica B **354**, 252 (2004).
[8]A. Lauchli and D. Poilblanc, Phys. Rev. Lett. **92**, 236404 (2004).
[9]C. Waldtmann, H.-U. Everts, B. Bernu, C. Lhuillier, P. Sindzingre, P. Lecheminant, and L. Pierre, Eur. Phys. J. B **2**, 501 (1998).
[10]J. Reuther, P. Wolfle, R. Darradi, W. Brenig, M. Arlego, and J. Richter, Phys. Rev. B **83**, 064416 (2011).
[11]P. W. Leung and N. W. Lam, Phys. Rev. B **53**, 2213 (1996).
[12]C. L. Kane, P. A. Lee, and N. Read, Phys. Rev. B **39**, 6880 (1989).
[13]G. Martinez and P. Horsch, Phys. Rev. B **44**, 317 (1991); Z. Liu and E. Manousakis, *ibid.* **45**, 2425 (1992).
[14]J. Ferrer, Phys. Rev. B **47**, 8769 (1993).
[15]J. Villain, J. Phys. (Paris) **38**, 26 (1977).
[16]J. Richter and J. Schulenburg, Eur. Phys. J. B **73**, 117 (2010), and references therein.
[17]L. Capriotti and S. Sachdev, Phys. Rev. Lett. **93**, 257206 (2004).
[18]E. Rastelli and A. Tassi, Phys. Rev. B **46**, 10793 (1992).
[19]I. J. Hamad, A. E. Trumper, A. E. Feiguin, and L. O. Manuel, Phys. Rev. B **77**, 014410 (2008).
[20]I. J. Hamad, L. O. Manuel, G. Martinez, and A. E. Trumper, Phys. Rev. B **74**, 094417 (2006).
[21]D. Poilblanc, A. Läuchli, M. Mambrini, and F. Mila, Phys. Rev. B **73**, 100403(R) (2006); I. J. Hamad, L. O. Manuel, and A. E. Trumper, Physica B: Phys. Condens. Matt. **404**, 2858 (2009).
[22]M. Takahashi, Phys. Rev. Lett. **58**, 168 (1987); Phys. Rev. B **40**, 2494 (1989).
[23]N. Read and S. Sachdev, Phys. Rev. Lett. **66**, 1773 (1991); S. Sachdev and N. Read, Int. J. Mod. Phys. B **5**, 219 (1991).
[24]S. Takei, C. H. Chung, and Y. B. Kim, Phys. Rev. **70**, 104402 (2004).